Effect of interwall surface roughness correlations on optical spectra of quantum well excitons

I. V. Ponomarev,* L. I. Deych, and A. A. Lisyansky
Department of Physics, Queens College of the City University of New York, Flushing, New York 11367 USA
(Received 20 March 2004; revised manuscript received 13 January 2005; published 5 April 2005)

We extend a theory of well-width fluctuations for inhomogeneous exciton broadening in quantum wells by expressing the fluctuation of the width in terms of the statistical characteristics of the morphological roughnesses of each interface forming the well. This allows us to take into account a possibility of cross correlations between the interfaces. We show that these correlations strongly suppress a contribution of interface disorder to the inhomogeneous linewidths of excitons. We also demonstrate that the vertical cross correlations are crucial for explaining the variety of experimental data on the dependence of the linewidth upon thickness of the quantum well.

DOI: 10.1103/PhysRevB.71.155303 PACS number(s): 68.35.Ct, 71.35.Cc, 78.67.De

I. INTRODUCTION

Absorption and luminescence exciton spectroscopy are among the most important tools for studying quantum wells (QWs) as well as other semiconductor heterostructures. Therefore, one of the most fundamental problems in the physics of these systems is establishing connections between the spectral line shapes and the microscopic properties of the respective structures. A great deal of effort was devoted to this problem over the last half of the 20th century, and it has been established that at low temperatures the exciton linewidth in absorption and photoluminescence spectra in quantum wells is predominantly inhomogeneous.[1] The shapes of the spectra in this case are determined by various types of disorders present in a structure, and it is currently generally accepted that the spectral widths in QWs are directly related to the quality of the interfaces, so that the luminescence spectra provide a quick and simple quality-assurance tool for QW growth.[2] However, as it will be seen in this paper, in spite of all the efforts, the existing theories of the inhomogeneous broadening of excitons in QWs still cannot satisfactorily explain all the diverse experimental data collected in this area.

The current theoretical approaches of interface-roughness effects on photoluminescence (PL) and absorption spectra in QWs are usually based on the concept of well-width fluctuation.[2–6] According to this theory a small fluctuation δL of QW width results in the fluctuation of the confinement electron and hole energies: $\delta E_n \sim (\partial E_n/\partial L)\delta L$. Therefore, the inhomogeneous broadening is proportional to the statistical average $\langle \delta E_n \rangle$ over all possible topological configurations. Despite a qualitative success in the prediction of the major exciton characteristics in PL and absorption spectra, this theory suffers from a lack of ability to fit the whole variety of the experimental data. (See a comparison of the theory well-width fluctuations with experiments in Sec. II). Also, the concept of a locally varying well width *implicitly* assumes that the surface corrugations of two QW interfaces are statistically independent, and can, therefore, be described by a single random function δL. However, there exists much evidence that this assumption does not correspond to realistic quantum well structures, in which the "vertical" correlations between two interfaces (when the later-grown interface "remembers" the profile of the first-grown interface) are present. One can mention, for instance, direct morphological analysis done with cross-sectional scanning tunnel microscopy,[7] scattering ellipsometry,[8] and x-ray reflection measurements.[9,10] Another relevant example of such correlations is the vertical stacking of quantum dots,[11] where vertical correlation length is observed up to an 80-monolayer thickness. The well-width fluctuation theory cannot describe an effect of these correlations on the exciton linewidths.

The goal of this paper is to develop a generalized theory, which would be able not only to clarify the importance of *interwall correlations*, especially for narrow QWs, but could also provide tools to deal with more complicated systems such as asymmetric QWs or superlattices. We explicitly show here that the presence of interwall correlations significantly modifies optical spectra, and that taking these correlations into account is necessary in order to achieve even a qualitative agreement between the theory and the experimental results. One of the important practical conclusions of this work is that narrow lines do not always mean a good-quality interface (which is often assumed in experimental publications), but can be the result of a line-narrowing effect due to the interwall correlations.

This paper is organized in the following way. In the Sec. II we shall provide a brief review and critical analysis of the existing experimental results and relevant theories. In Sec. III we will generalize the earlier theories of interface disorder[2–6] to include the effects of the vertical correlations. In the Sec. IV we will compare the results of our analysis with experiments. (For comparison of our theory with the theory of local width fluctuations see discussions at the end of Sec. III A). The paper is concluded by an Appendix, in which we comment on the role of the lateral (in-plane) correlation length in the optical spectra of QW.

II. COMPARISON BETWEEN CURRENT THEORIES AND EXPERIMENT: CRITICAL REVIEW

Since a QW is generally a heterostructure formed by a binary semiconductor (AB) and a ternary disordered alloy ($AB_{1-x}C_x$), there are two types of disorders responsible for

the inhomogeneous broadening. One is compositional disorder caused by concentration fluctuations in a ternary component of the QW as well as random diffusion across the interface.[12,13] The other source of inhomogeneous broadening in QWs is associated with the roughness of the interface caused by the formation of monolayer islands at the interfaces, resulting in local changes in the well thickness.[2–6] The quality of the interfaces is very sensitive to the ambient parameters of the growth process. Depending on growth conditions, the atoms deposited on the surface can form "islands" of various lateral sizes with different correlation scales. These morphological changes manifest themselves in the shape and width of the optical spectra of QW excitons. Since both types of disorders can be ultimately traced to local changes in concentration, an accurate distinction between them is not a trivial task, and it was first elucidated in Ref. 3.

Theoretical studies of effects due to compositional and interface disorders on absorption and photoluminescence spectra have a long history (for review articles see, for example, Refs. 1, 14, and 15 and references therein.). In general, absorption and photoluminescence spectra, apart from the Stokes shift, have also different lineshapes. The calculation of the exciton absorption line shape is equivalent in the dipole approximation to the estimation of the optical density function[1] $A(\varepsilon)$ which is determined by the properties of the underlined random potential. In turn, the emission peak should be treated as a more complicated average over only partially thermalized exciton occupation numbers. Below we concentrate on calculation of the exciton absorption peak. This problem can be divided into two fairly independent parts. The first deals with the derivation of the random potentials acting on excitons in QWs from the properties of microscopic fluctuating parameters (concentrations, well thickness, etc.). Its main objective is to calculate the correlation functions of these potentials. The second part of the problem consists of calculations of the characteristics of excitons subjected to these potentials and in establishing relations between the characteristics of optical spectra (linewidth, shape) and the properties of the potentials [root-mean-square (rms)] fluctuation and correlation length). Both of these problems were carefully studied in the past, but since the focus of the present work is on the former, we shall discuss it in more detail.

The main object of our discussion is the rms value of the random potentials W, defined as $W=\sqrt{\langle V_{eff}(\mathbf{R})^2\rangle}$, and its dependence on the microscopic parameters of the QW. Here V_{eff} is the effective potential acting on excitons due to both compositional and interface disorders. The current theories[3,13] predict distinctly different properties for contributions to the potential from these two types of disorders. These properties can be devised from the behavior of the single-particle electron and the hole QW wave functions. In particular, the dependence of W upon the width of the well L for a narrow well is predicted as being $\propto L$ for the interface disorder. For the compositional disorder, it depends on whether the QW is formed by a ternary alloy or a binary system.[13] In the former case (as in $In_xGa_{1-x}As/GaAs$) $W \propto L^{3/2}$, while in the case in which the QW is formed by a binary material, the dependence is $W\propto\sqrt{L}$. In the three-dimensional limit $L\to\infty$ the contributions of the two types of disorders to $W(L)$ are also different. The contribution of the interface disorder for large L decreases as $1/L^3$, while the role of the alloy disorder again depends upon the type of the structure. If QW is formed by a ternary alloy W decreases with the width only weakly, as $1/\sqrt{L}$, before reaching a constant three-dimensional limit. If, however, the alloy forms barriers, W decreases with L much faster as $\exp(-\kappa_0 L)/L^3$, where κ_0 is an inverse penetration length of ground-state wave function in the barrier region. Although in both cases the function $W(L)$ has a maximum at some intermediate values of L, the position of the maximum and the shape of the function $W(L)$ differ for the two types of disorders.

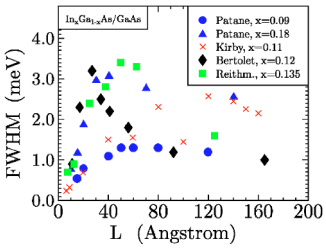

FIG. 1. Experimental dependences of the low-temperature exciton's full width half maximum (FWHM) on the QW average size, L. All the data are presented for the $In_xGa_{1-x}As/GaAs$ QW's. The results were taken from the following references: Patanè *et al.* (Ref. 16), Kirby *et al.* (Ref. 17), Bertolet, *et al.* (Ref. 18), and Reithmaier *et al.* (Ref. 19).

While the qualitative picture of disorder-induced broadening is understood rather well, attempts at a quantitative comparison of the theoretical predictions with the experiments face significant difficulties. In Fig. 1 we collected experimental data for the dependencies of low-temperature photoluminescence exciton linewidths on QWs of average thickness, L. All of the data are for $In_xGa_{1-x}As/GaAs$ heterostructures and represent experimental results from several research groups.[16–19] While all the results show a nonmonotonous dependence in accord with theoretical expectations, the maxima have different positions and do not seem to have a regular dependence on the concentration; the peak for $x=0.18$ lies between the peaks for $x=0.12$ and $x=0.135$. The maxima also have different heights and sharpness. For example, the fullwidths at half maximum (FWHM) for $x=0.09$ and $x=0.11$ have very smooth behaviors more characteristic of compositional disorder, while other data have rather sharp features more typical of interface disorder. Finally, the values of FWHM at large L, which are determined mainly by compositional disorder, are scattered over quite a broad range.

It is not surprising that different samples show different behaviors in Fig. 1, since they were prepared under different growth conditions, and, as a result, they have different alloy disorder and interface-roughness characteristics. It is more surprising that if we try to analyze these data in light of the current theories[3,13] of interface-roughness and alloy-disorder inhomogeneous broadening, then we encounter difficulties in fitting all these curves with the parameters in hand. Regarding the alloy contribution to the linewidth, we note that in the quantum mechanical approaches to this problem[3,12,13,20] this

contribution is completely determined by the alloy concentration and QW width; the theories do not contain any unknown parameters that could be used to fit the theoretical predictions to the experiments. Therefore, one can directly compare the theoretical predictions with the experimental results using the large L asymptote of the linewidth. The initial calculations for the alloy-induced disorder in the bulk[12,21] and in the quantum wells[13] were done in the adiabatic approximation, where the Bohr's radius of an exciton a_B was assumed to be much larger than a correlation length of the effective potential ℓ_c. If one applies that theory[13] to the case of an $In_{0.12}Ga_{0.88}As/GaAs$ QW, the FWHM comes out to be equal to 0.36 meV for $L=150$ Å. This value is much smaller than the observed bulk value.[38] The same order of magnitude results are obtained in the semiclassical limit of the theory[22,23] with the Gaussian shape of the exciton linewidth. One can reasonably argue[1] that the adiabatic approximation fails for a heavy hole and a light electron ($m_h \gg m_e$), both being subject to short-range energy fluctuations. Even for the underlying "white-noise" disorder, the effective potential felt by an exciton has two different correlation lengths. A rather massive hole will average only a small volume around the center of mass (COM) of the exciton, whereas a light electron is spread out over a much larger area of the order of a_B^2. As a result, the hole will be much more sensitive to compositional fluctuations, and its contribution to the effective disorder potential will be enhanced by the factor (M/m_e),[2] where $M=m_e+m_h$. However, the linewidths found using the improved theories[3,20] turn out to be much larger than the experimental results (see also Fig. 8 below). Thus, existing theories cannot produce an accurate result for the alloy-disorder contribution to the exciton linewidth.

It is less straightforward to compare the theory with the experiments for interface-roughness-induced broadening because it is difficult to separate the contributions from the two types of disorders in the regime of the small and intermediate values of L. One could hope to identify the most important contribution by the slope of the $W(L)$ dependence at small L, but, unfortunately, the accuracy of the existing data does not allow one to distinguish between the L or $L^{3/2}$ dependencies. The manifestation of the interface disorder in optical spectra is clearer in the case of systems in which growth interruption resulted in the formation of sufficiently large, monolayer islands. It was shown in Ref. 6 that these islands could be responsible for the observed splitting of the exciton spectra. Also, interface roughness has been studied directly by such experimental techniques as microphotoluminescence, cathodoluminescence, transition electron microscopy, or scanning tunneling microscopy.[2,5,14,16–19,24–27]

The diversity of the experimental behavior for the FWHM shown in Fig. 1 presents a significant difficulty for the existing theories of the interface contribution to the linewidth,[3,28] even from the point of view of the qualitative interpretation of the results. Indeed, the statistical properties of an interface are usually characterized by two length parameters: the thickness fluctuation h and the lateral (in-plane) correlation length $\sigma_\perp$. With some reservations they are often taken to be equivalent to the average height and the lateral size of the islands at the interface. The size of the height fluctuations h usually has a very restricted range of variations of one or two

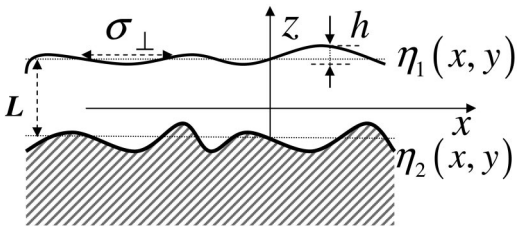

FIG. 2. Characteristic length scales describing the interface roughness of a QW.

monolayers. In the semiclassical limit of the Gaussian-shaped linewidth, the broadening is proportional to the product $h\sigma_\perp$, which is really only one flexible parameter of the theory. With the help of this parameter it is possible to adjust the relative heights of the maxima, but not their positions and particularly not the sharpness of these maxima. Even if one takes into account the contributions from both types of disorders, it is still not possible to explain the variations between the optical spectra of different samples, a problem addressed in Sec. IV.

It is clear from the provided analysis that the existing theories of the inhomogeneous broadening of excitons are unable to quantitatively explain the experimental data. We suggest in this paper that one of the reasons for this failure is the neglect of the interwall correlations mentioned in the Introduction. While this idea does not fix the problems caused by wrong estimates of the alloy-disorder contribution, we will show in the subsequent sections of this paper that it does allow us to explain all varieties of experimental results related to the properties of the curves in Fig. 1 in the vicinity of their maxima.

III. STATISTICAL PROPERTIES OF THE INTERFACES AND EXCITON EFFECTIVE POTENTIAL

A. A model of the interface disorder

In order to make the problem tractable, we introduce standard simplifications assuming that both conduction and valence bands are nondegenerate and that they both have an isotropic, parabolic dispersion characterized by the masses m_e and m_h, respectively. Throughout the paper we use effective atomic units (a.u.), which means that all distances are measured in the units of the effective Bohr radius $a_B=\hbar^2\epsilon/\mu^* e^2$, energies in units of $E_{a.u.}=\mu^* e^4/\hbar^2\epsilon^2 \equiv 2\mathrm{Ry}$, and masses in units of reduced electron-hole mass μ^*, where $1/\mu^*=1/m_e^*+1/m_h^*$. In this notation $m_{e,h}=m_{e,h}^*/\mu^*$, where $m_{e,h}^*$ are the effective masses of an electron and a heavy hole. We will choose the z axes in the direction of growth of the structure (vertical direction). The plane perpendicular to this direction is the lateral plane (see Fig. 2). We measure the electron and hole energies in the QW from the conduction and valence band edges of the barrier, respectively. Then the potential of a QW with interface roughness is given by

$$U_{e,h}(\mathbf{r}) = -V_{e,h}(\theta[z+L/2-\eta_1(x,y)]-\theta[z-L/2-\eta_2(x,y)]) \approx U_{e,h}^{(0)}(z)+\delta U_{e,h}^{\mathrm{int}\,f}(\mathbf{r}), \quad (1)$$

where $\theta(z)$ is a step function, $V_{e,h}$ are differences in the offset band energies, and

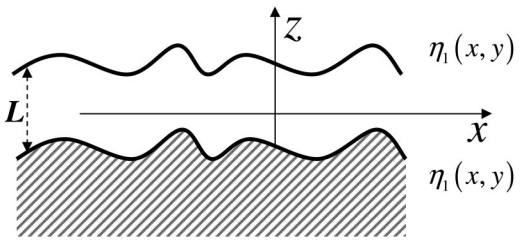

FIG. 3. The limiting case of the absolutely correlated interfaces, $\eta_1 = \eta_2$.

$$U_{e,h}^{(0)}(z) = -V_{e,h}[\theta(z+L/2) - \theta(z-L/2)], \tag{2}$$

$$\delta U_{e,h}^{\text{int}\,f}(\mathbf{r}) = V_{e,h}[\eta_1(x,y)\delta(z+L/2) - \eta_2(x,y)\delta(z-L/2)]. \tag{3}$$

The random functions $\eta_{1,2}(x,y)$, with zero mean, characterize the deviation of the ith interface from its average position. The perturbation expansion of the θ function is justified because an interface roughness is almost always small for the typical parameters in semiconductor heterostructures. The presence of the two functions $\eta_{1,2}(x,y)$ distinguishes Eq. (2) and Eq. (3) from the respective equations of Ref. 3, where the roughness of only one interface was taken into account.

The statistical properties of the interfacial roughness in multilayered systems can be characterized by the height-height correlation functions,

$$\langle \eta_i(\boldsymbol{\rho}_1)\eta_j(\boldsymbol{\rho}_2)\rangle = h^2 f_{ij}\zeta(|\boldsymbol{\rho}_1 - \boldsymbol{\rho}_2|), \tag{4}$$

where h is an average height of interface inhomogeneity, and $\langle\cdots\rangle$ denotes an ensemble average. We assume here that the dependence of both the diagonal and the nondiagonal correlations on the lateral coordinates $\boldsymbol{\rho}$ is described by the same function $\zeta(\boldsymbol{\rho})$. The diagonal elements f_{ii} are the constants, and the respective functions describe the lateral correlation properties of a given interface (*self-correlation functions*). The non-diagonal elements with $i \neq j$ introduce correlations between different interfaces; the respective quantity $f_{12}(L/\sigma_{||})$, which can be called a *cross-* or *vertical-correlation function*, is a function of the average width of the well and is characterized by the vertical correlation length $\sigma_{||}$. (A subscript "||" denotes that the direction of the vertical correlation is parallel to the direction of growth.)

The effect of the interwall vertical correlations has been previously considered in studies of the conductivity of thin metallic films.[29–31] To the best of our knowledge, in all previous microscopic studies of the exciton line shape in the optical spectra of QWs, these correlations were omitted. Such an approximation is valid for wide QWs, but in the case of narrow QWs the vertical correlations are experimentally confirmed[7–11] and should be taken into account. In the limit $L/\sigma_{||} \ll 1$ it is reasonable to assume that $f_{11} = f_{22}$ and that the interwall correlation function f_{12} tends to $(f_{11} + f_{22})/2$, which means that for the very small separation between the interfaces one random surface spatially repeats the pattern of the other (see Fig. 3). As we shall see below, the effect of the interface disorder in this case tends to cancel out at least in the first order of the perturbation theory. For the sake of concreteness we will assume below that

$$2f_{12} = (f_{11} + f_{22})\exp(-L^2/\sigma_{||}^2). \tag{5}$$

The value of the vertical correlation length $\sigma_\perp$ depends on the growth process. In the following analysis we will also assume the Gaussian form for the lateral correlation function:

$$\zeta(\mathbf{R}) = \exp(-R^2/2\sigma_\perp^2). \tag{6}$$

The limit $\sigma_\perp \to 0$ corresponds to the white-noise correlator,

$$\zeta(\mathbf{R}) = 2\pi\sigma_\perp^2\,\delta(\mathbf{R}). \tag{7}$$

Following the standard procedure[12] described in numerous papers we derive the Schrödinger equation for the center-of-mass (COM) exciton motion subjected to an effective random potential,

$$\left[-\frac{\Delta_{\mathbf{R}}}{2M} + U_{eff}(\mathbf{R})\right]\psi_i(\mathbf{R}) = \varepsilon_i\psi_i(\mathbf{R}), \tag{8}$$

with $U_{eff}(\mathbf{R})$ given by

$$U_{eff}(\mathbf{R}) = \int (\delta U_e + \delta U_h)\phi^2(\boldsymbol{\rho})\chi_e^2(z_e)\chi_h^2(z_h)d^2\rho dz_e dz_h \equiv U_e(\mathbf{R}) + U_h(\mathbf{R}), \tag{9}$$

where $\delta U_{e,h}$ are defined in Eq. (3), $\boldsymbol{\rho} = \boldsymbol{\rho}_e - \boldsymbol{\rho}_h$, and $\mathbf{R} = (m_e\boldsymbol{\rho}_e + m_h\boldsymbol{\rho}_h)/M$. For the symmetric QWs, $\chi(-L/2) = \chi(L/2)$, and from Eq. (3) we obtain

$$U_{e,h}(\mathbf{R}) = V_{e,h}\chi_{e,h}^2(L/2)\int [\eta_1(\mathbf{R} \pm \beta_{h,e}\boldsymbol{\rho}) - \eta_2(\mathbf{R} \pm \beta_{h,e}\boldsymbol{\rho})]\phi^2(\boldsymbol{\rho})d^2\rho. \tag{10}$$

Here $\beta_{h,e} = m_{h,e}/M$. Hereafter we will omit an explicit dependence on L for the electron and hole wave functions $\chi_{e,h}^2(L/2)$, always assuming that their values are taken at the position of the interface. The correlation function for the effective potential $U_{eff}(\mathbf{R})$ can then be expressed as

$$\langle U(\mathbf{R}_1)U(\mathbf{R}_2)\rangle \equiv T_{ee} + T_{hh} + 2T_{eh}, \tag{11}$$

where

$$T_{ii} = h^2V_i^2\chi_i^4[f_{11} + f_{22} - 2f_{12}(L)] \times \int d^2\rho d^2\rho'\,\phi^2(\rho)\phi^2(\rho')\zeta(|\mathbf{R} - \beta_j(\boldsymbol{\rho} - \boldsymbol{\rho}')|), \tag{12}$$

$$T_{eh} = h^2V_eV_h\chi_e^2\chi_h^2[f_{11} + f_{22} - 2f_{12}(L)] \times \int d^2\rho d^2\rho'\,\phi^2(\rho)\phi^2(\rho')\zeta(|\mathbf{R} - \beta_h\boldsymbol{\rho} + \beta_e\boldsymbol{\rho}'|), \tag{13}$$

where $i,j = e$ or h and $\mathbf{R} = \mathbf{R}_1 - \mathbf{R}_2$.

In all of these expressions, the terms in front of the integrals determine the dependence of the correlation function on the QW width L, while the integrals themselves determine

the spacial correlations in the lateral dimensions. Each of these terms can be presented in the form

$$T_{ij}(L,R) = h^2 V_i V_j F_{ij}(L) G_{ij}(R), \tag{14}$$

$$F_{ij}(L) = \chi_i^2 \chi_j^2 [f_{11} + f_{22} - 2f_{12}(L)], \tag{15}$$

$$G_{ij}(R) = \int d^2\rho d^2\rho' \phi^2(\rho)\phi^2(\rho')\zeta(|\mathbf{R} - \beta_j\boldsymbol{\rho}' + \beta_i\boldsymbol{\rho}|), \tag{16}$$

where the indexes i,j take the values e and h. (Note that the order of these indices in the integrand is important.)

Equations (14)–(16) can be considered as an extension of an often-used theory of well-width fluctuations.[3] According to this theory the width of a QW is given by $\mathcal{L}=\langle L\rangle+\delta L$, where δL is a random variable with a correlator $\langle \delta L(\boldsymbol{\rho}_1)\delta L(\boldsymbol{\rho}_2)\rangle = 2h^2 \exp(-|\boldsymbol{\rho}_1-\boldsymbol{\rho}_2|^2/2\sigma_\perp)$. Our approach introduces independent roughnesses for each of the two interfaces η_1 and η_2 so that $\delta L=\eta_1-\eta_2$. This results in the additional independent statistical parameters f_{ij} and $\sigma_{||}$. In the first order of the perturbation theory, in the case of a symmetrical (equal potential heights) QW both approaches can be reconciled by a proper choice of the correlation function $\langle \delta L(\boldsymbol{\rho}_1)\delta L(\boldsymbol{\rho}_2)\rangle$ for the QW-width fluctuations. However, already in the second order of the perturbation theory the presented approach differs qualitatively from the approach of Ref. 3. An easy way to see the difference is by considering the limit of the absolutely correlated (parallel) interfaces (see Fig. 3) $\eta_1=\eta_2$. Now, $\delta L\equiv 0$, and the interface-roughness contribution in the theory of well-width fluctuations vanishes completely. In our approach, the result is zero, $F_{ij}(L)=0$, only in the first order of the perturbation expansion. The second order brings "mixing" of the z and in-plane coordinates: $\langle \boldsymbol{\nabla}\eta_1(\boldsymbol{\rho})\boldsymbol{\nabla}\eta_1(\boldsymbol{\rho}')\chi\chi''\rangle \propto h^2/(L\sigma_\perp)^2$ and similar terms. (These results will be published elsewhere.) Corrections of this type can play an essential role for a not very smooth surface corrugation. Also, the advantage of the multiple interface-roughness approach is that it can be easily extended to the more complicated cases of an asymmetric QW, a QW in the external fields, or multiple QWs and superlattices, where a right guess for the width-fluctuation correlator is not so obvious.

Another apparent difference of Eq. (15) from the results of Ref. 3 is that the interface disorder potential is determined there by the derivative of the locally varying confinement energy, but it does not depend on the value of the electron and hole wave functions at the interfaces. These results can be easily reconciled after using Ehrenfest's theorem,

$$\frac{\partial E_{h,e}}{\partial L} = \left\langle \chi_{h,e} \left| \frac{\partial \hat{H}_{h,e}}{\partial L} \right| \chi_{h,e} \right\rangle = \langle \chi_{h,e} | \delta U^{\text{int}\,f}_{h,e}(\mathbf{r}_{h,e}) | \chi_{h,e} \rangle,$$

where $\delta U^{\text{int}\,f}$ is given by Eq. (3). In the more general cases, in which the confinement energy depends on more than one parameter, a perturbation theory leaves the only consequent choice of expressing the interface disorder potential through the values of the corresponding wave functions on the interfaces.

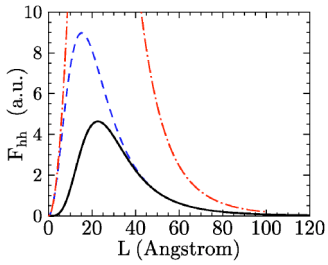

FIG. 4. Dependence of the correlation function of the hole-hole interface-roughness potential on the well width in an $In_{0.12}Ga_{0.88}As/GaAs$ QW. The solid line is the function $F_{hh}(L)$. The dashed line is the fourth degree of the hole wave function at the interface. The dot-dashed line shows the approximations of this function for small and large L, given by Eqs. (19) and (20). The maximum of $\chi_h(L)^4$ is approximately located at $1/\kappa_{0h}=1/\sqrt{2m_hV_h}$.

B. Dependence on well thickness

Let us first focus on the functions $F_{ij}(L)$, which determine the dependence of the total correlation function on the QW width L. For the sake of concreteness we consider in detail the function F_{hh}. The analysis of the other functions is similar. The dependence of F_{hh} on L comes from two factors. The first factor is the 4th degree of the electron's QW wave function χ_h^4 calculated at the interfaces, $z=\pm L/2$. This dependence in the $In_{0.12}Ga_{0.88}As/GaAs$ QW is shown in Fig. 4 by a dashed line. It is easy to understand the behavior of χ_h^4 for the cases of large and small widths. The characteristic scale here is given by $1/\kappa_{0h}=1/\sqrt{2m_hV_h}$, since this scale determines the number of energy levels in a finite QW ($N=1+[\kappa_h L/\pi]$).

For a finite QW the ground-state wave function has a piecewise form,

$$\chi(z) = \begin{cases} A\cos(kz), & z \leqslant |L/2| \\ B\exp(-\kappa|z|), & z \geqslant |L/2|, \end{cases} \tag{17}$$

where $\kappa=\sqrt{\kappa_0^2-k^2}$, and k is the ground-state wave vector. From the normalization and matching conditions, one can readily obtain the value of the square of the wave function at the interface

$$\chi^2 = B^2\exp(-\kappa L) = \left[\frac{\kappa}{1+\kappa^2/k^2+\kappa L\kappa_0^2/(2k^2)}\right]. \tag{18}$$

In the case of a wide QW, there are many discrete levels in the well, and the well is "almost infinite:" $k\approx\pi/L-2\pi/L^2\kappa_0$, $\kappa\approx\kappa_0$, and

$$\chi^2 \approx \frac{2\pi^2\kappa_0}{\kappa_0^3L^3+2\kappa_0^2L^2+2\pi^2} \sim \frac{1}{L^3}. \tag{19}$$

Since for large well widths the vertical interwall correlations are negligible, $f_{12}\to 0$, Eq. (19) determines the total decrease of the interface correlator with increasing width.

In the opposite case of very narrow QWs, there is only one shallow level, which can be determined from the δ-functional potential approximation: $k\approx\kappa_0-L^2\kappa_0^3/8$, $\kappa\approx\kappa_0^2L/2$, and

$$\chi^2 \approx \frac{\kappa_0^2 L}{2}. \tag{20}$$

If one neglects vertical correlations, this expression describes the suppression of the interface disorder for narrow wells because of a decreased portion of the hole (electron) wave function inside the well. This result was obtained earlier in, for instance, Ref. 22. Interwall correlations, however, significantly modify this dependence. For lengths smaller than the vertical correlation length $\sigma_{||}$ we have

$$f_{11} + f_{22} - 2f_{12} \sim \left(\frac{L}{\sigma_{||}}\right)^{\gamma}, \tag{21}$$

where γ is determined by the form of the interwall correlation factor f_{12}. For example, for Gaussian or Lorentzian dependences of $f_{12}(L)$, the parameter $\gamma=2$, while for the exponential form of this function $\gamma=1$. Thus we obtain that, in narrow QWs, interface correlations are strongly suppressed by the factor,

$$F_{ij}(L) \sim L^{2+\gamma}, \quad L < \sigma_{||}, 1/\kappa_0. \tag{22}$$

While the transition between the two asymptotic behaviors of χ is determined by the parameter κ_0, the behavior of f_{12} depends on the correlation length $\sigma_{||}$, which is a completely independent parameter. The experimental data suggest that it is quite possible for $\sigma_{||}$ to be much larger then κ_0. In this case, interwall correlations can affect not only the $L \to 0$ asymptotic of W, but also its behavior at $L \gg \kappa_0$. Instead of $1/L^3$ behavior one would have a much slower decrease of W with L, $W \propto L^{\gamma-3}$.

From the behavior of the wave function (18) we can see that the maximum of $F_{hh}(L)$ is reached in the vicinity of $L \sim 1/\kappa_{0h}$. However, as the previous analysis demonstrates, the vertical correlation function f_{12} can significantly shift this position; it can also change the height and shape of the peak. Thus, the presence of the interwell correlation term $f_{11}+f_{22}-2f_{12}$ in the function F_{hh} can naturally explain all variety of experimental results related to the properties of the curves in Fig. 1 in the vicinity of their maxima. The graph of function F_{hh}, with interwall correlations taken into account, is shown in Fig. 4. One can see that these correlations indeed significantly affect the shape of this function. While we only discussed the properties of the hole-hole correlator, it is clear that the behavior of the electron-electron and hole-electron terms is similar.

C. Dependence on lateral correlation length

In order to investigate the results of the interplay between the lateral and interwall correlations, let us now analyze the lateral correlation functions $G_{ij}(R)$. Their behavior is determined by the ratio of the potential correlation length $\sigma_\perp$ to the average size of the exciton in a plane, as well as by dimensionless parameters β_e and β_h. In order to evaluate the respective integrals, we chose the normalized ground-state function of the exciton relative motion in a quasi-two-dimensional form,[32]

$$\phi(\rho) = \sqrt{\frac{2}{\pi\lambda^2}} \exp(-\rho/\lambda), \tag{23}$$

where λ is a variational parameter that indicates the average exciton size.

For the ground state function, Eq. (23), and the height-height correlation function, Eq. (6), the lateral dependence of the correlator $G_{ij}(R)$ can be presented as a function of two parameters $G_{ij}(R) \equiv G_{ij}(R; y_j, \alpha)$, where

$$y_i = \frac{\sqrt{2}\sigma_\perp}{\beta_i \lambda}, \tag{24}$$

and $\alpha = \min(\beta_i, \beta_j)/\max(\beta_i, \beta_j)$. The parameter α is equal to unity for the electron-electron and the hole-hole correlator. For the cross term G_{eh} this parameter is equal to m_e/m_h, which is much less than unity for the majority of the semiconductor materials. This fact allows for additional simplifications when evaluating the integrals. The parameter $y_{e(h)}$ defines the ratio of the renormalized lateral correlation length $\beta_{e(h)}\lambda$ of the effective hole (electron) potential to the original correlation length of the interface fluctuations. For holes with $m_h \gg m_e$ this renormalized correlation length is much smaller than the corresponding length for the electrons. The latter implies that the interface disorder has a bigger impact on the holes than on the electrons. This is also true for the contribution of the alloy disorder to the broadening.[12] Thus, the lateral correlation function can be rewritten in the following form:

$$G_{ij}(R; y_j, \alpha) = \frac{4y_j^4}{\alpha^2\pi^2} \int d^2\rho d^2\rho' \exp[-2y_j(\rho' + \alpha^{-1}\rho)] \times \exp(-|\mathbf{R} - \boldsymbol{\rho}' + \boldsymbol{\rho}|^2). \tag{25}$$

We shall focus on its value at the origin $G_{ij}(0; y_j, \alpha)$ which determines the variance of the potential W. The expression for W in this case can be presented in the following form:

$$W^2 = h^2[f_{11} + f_{22} - 2f_{12}][V_h^2\chi_h^4 G_{hh}(0; y_e, 1) + 2V_eV_h\chi_e^2\chi_h^2 G_{eh}(0; y_h, \alpha) + V_e^2\chi_e^4 G_{ee}(0; y_h, 1)]. \tag{26}$$

The calculations are easier for the cross term G_{eh}, because we can take advantage of the smallness of $\alpha \ll 1$,

$$G_{eh}(0; y_h, \alpha) = 4y_h^2 \int dtt \exp(-t^2 - 2y_h t) + O(\alpha^2) = 2y_h^2/(1 + \alpha)^2 - 2y_h^3 \exp(y_h^2)\sqrt{\pi}[1 - \mathrm{erf}(y_h)] + O(\alpha^2), \tag{27}$$

where $\mathrm{erf}(y)$ is the error function. The function (27) is shown in Fig. 5. It has the following behavior for small and large y:

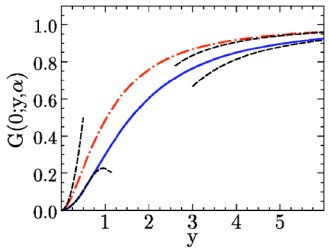

FIG. 5. The thick solid line is the lateral correlation function $G(0;y,1)$. The dashed lines are its asymptotes given by Eq. (31). The thick dotted-dashed line is a cross-term correlator $G(0;y,0)$. Its asymptotes (dashed lines) are given by Eq. (28).

$$G_{eh}(0;y_h,0) \approx \begin{cases} \dfrac{4\sigma_\perp^2}{\lambda^2} - 2\sqrt{\pi}y_h^3 + \cdots, & y_h \ll 1 \\ 1 - \dfrac{3}{2y_h^2}, & y_h \gg 1. \end{cases} \tag{28}$$

The calculations are more cumbersome for the electron-electron and the hole-hole contributions $G_{ii}(0,y_j,1)$. It is convenient to perform a transformation to the new set of coordinates which reflect the symmetry of the integral,[33]

$$s = \rho_1 + \rho_2, \quad t = \rho_1 - \rho_2, \quad u = \rho_{12} = \sqrt{\rho_1^2 + \rho_2^2 - 2\rho_1\rho_2 \cos\theta}. \tag{29}$$

After this transformation[39] the calculations for G_{ii} are reduced to the one-dimensional integral,

$$G_{ii}(0,y_j,1) = y_j^4 \int_0^\infty ds e^{-2y_j s}\left[s + (2s^2-1)e^{-s^2}\frac{\sqrt{\pi}\,\mathrm{erf}(is)}{2i}\right]. \tag{30}$$

The term in square brackets in the integrand of Eq. (30) is a smooth function that behaves as $\sim(8/3)s^3$ for small s and changes its behavior to $\sim 2s$ for $s>1$. These dependencies allow one to estimate the asymptotic behavior for the correlator $G_{ii}(0;y_j,1)$,

$$G_{ii}(0;y_j,1) \approx \begin{cases} \dfrac{y_j^2}{2} - \dfrac{23y_j^4}{84}, & y_j \ll 1 \\ 1 - 3/y_j^2, & y_j \gg 1. \end{cases} \tag{31}$$

The first terms in the series expansions of Eqs. (28) and (31) for small y correspond to the white-noise limit of the height-height correlation function, Eq. (7), and they were obtained previously in Ref. 34. They can be readily derived by the substitution of a δ function instead of the last exponent in the integrand of Eq. (25). The consecutive terms in these formulas describe deviations from the white-noise model in the case of the short-range correlations. The dependence of the correlators $G_{ij}(0;y,\alpha)$ on the respective parameters y_i is shown in Fig. 5, from which one can see that corrections to the white-noise approximation become significant, even at relatively small values of the correlation length, $\sigma_\perp$.

For the white-noise interface roughness, Eq. (7), the analytical results can be obtained for the more elaborate exciton ground-state trial function,[35]

$$\phi(\rho) = \frac{2\exp(\gamma)}{\sqrt{2\pi\lambda^2(1+\gamma)}} \exp\left(-\sqrt{\rho^2/\lambda^2 + \gamma^2/4}\right), \tag{32}$$

which more accurately takes into consideration the three-dimensional character of the exciton. The parameter $\gamma = 2d/\lambda$ determines the ratio of the finite average distance d between the electron and the hole in the QW to the two-dimensional Bohr radius λ. In this case, one can obtain for the most important hole-hole correlator ($\alpha=1$) the following expression:

$$G(0,\sigma_{||}, \quad \{\lambda,\gamma\},\beta,1) = \frac{\sigma_{||}^2}{\beta^2\lambda^2}\frac{1+2\gamma}{(1+\gamma)^2}. \tag{33}$$

This result formally coincides with the short-range limit $y^2/2$ of Eq. (31) after the introduction of the renormalized effective Bohr radius $\tilde{\lambda} = \lambda(1+\gamma)/\sqrt{1+2\gamma}$. Since the parameter γ in this expression is usually less than or of the order of unity, this renormalization is not significant, and we can conclude that an approximation of the exciton wave function by Eq. (23) gives reasonable results, at least for the short-range interface disorder. Collecting together all of the results for the variance, we obtain in the limit of the short-range interface disorder,

$$W^2 = h^2[f_{11} + f_{22} - 2f_{12}(L/\sigma_{||})]\frac{\sigma_\perp^2}{\lambda^2} \times \left[\frac{V_h^2\chi_h^4}{\beta_e^2} + 8V_eV_h\chi_e^2\chi_h^2 + \frac{V_e^2\chi_e^4}{\beta_h^2}\right]. \tag{34}$$

Apart from the vertical-correlation factor, $f_{11}+f_{22}-2f_{12}$, this expression coincides with the results obtained in Ref. 34. As expected, in the case in which holes have a significantly larger mass than electrons (the typical situation for the $In_xGa_{1-x}As/GaAs$ or $Al_xGa_{1-x}As/GaAs$ quantum wells), the hole-hole term in square brackets in Eq. (34) dominates. In the opposite limit of the long-range interface correlations the result is

$$W^2 = h^2[f_{11} + f_{22} - 2f_{12}(L/\sigma_{||})](V_h\chi_h^2 + V_e\chi_e^2)^2, \tag{35}$$

which agrees with the conclusion of Ref. 6 obtained for a different model of the interface disorder: in the regime of the long-range correlations the distribution of the effective potential reproduces the distribution of the interface roughness.

IV. COMPARISON WITH EXPERIMENTAL RESULTS

In order to compare the calculations of W with the experimental absorption spectra one needs to evaluate the dynamics of the excitons in a random potential with the given correlation properties. This problem was intensively discussed in the literature,[1,13,15,21] and we are going to use the results of the cited papers in conjunction with our analysis of the effective potential. There are two main models of exciton dynamics in a random model. One of them treats excitons quantum-mechanically in the limit of negative and large energies, while describing a most important intermediate region using an interpolation procedure.[13,21] In this approach the

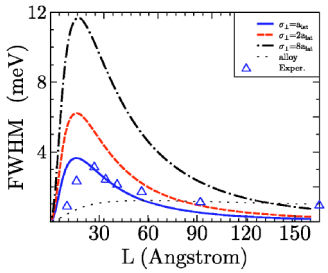

FIG. 6. Dependence of the interface-roughness-induced broadening on the perpendicular correlation length ("island size") $\sigma_\perp$. The correlation length is given in terms of a number of lattice constants (a_{lat}=5.869 Å). For all curves the composition concentration is x=0.12, and the vertical correlation length parameter is fixed by $\sigma_{||}=a_{lat}$. The dotted line is the rescaled alloy disorder contribution. The experimental data, shown by triangles, are taken from Ref. 18 and are presented here for comparison only.

absorption line has an asymmetric shape with the linewidth proportional to W^2. In the second approach excitons are treated semiclassically;[1] if the underlying compositional or interface-roughness disorder is described by the Gaussian random process, then the shape of the exciton line is also approximately Gaussian with a FWHM equal to $\Delta=2\sqrt{2\ln(2)}W$. A transition between the quasiclassical and quantum regimes of exciton dynamics is determined by the parameter $\nu=W/K_c$. Here $K_c=\hbar^2/2M\ell_c^2$ is the kinetic energy of an exciton confined in a spatial region of size ℓ_c, where ℓ_c is a suitably defined correlation length of the random potential[15] (also see the Appendix). The quantum limit corresponds to the case $\nu\lesssim 1$, while the semiclassical approximation is valid when $\nu\gg 1$.

In order to compare the results obtained here with optical experimental data, we will make use of the semiclassical theory of exciton absorption, which, according to Ref. 15, can be reliably applied to the situation under consideration. (The typical material parameters for an $In_xGa_{1-x}As/GaAs$ QW yield $\nu\sim 5$ for $\sigma_\perp=2a_{lat}$, where a_{lat}=5.87 Å is a lattice constant and ν increases with an increase of the correlation length.) Using the semiclassical relation for Δ, we plot the dependence of the interface-roughness contribution to the exciton linewidth as a function of the well width in Figs. 6 and 7. Figure 6 represents curves for different lateral correlation lengths ("island sizes"), while Fig. 7 shows how these results are modified by the interwall correlations. The first thing to notice is that the changes in the lateral correlation length

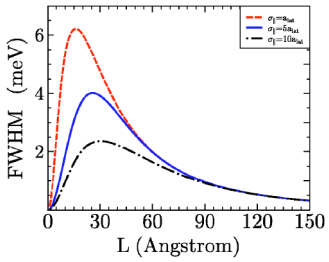

FIG. 7. Dependence of the interface broadening on the vertical correlation length ("island size") $\sigma_{||}$. All curves are drawn for $\sigma_\perp=2a_{lat}$.

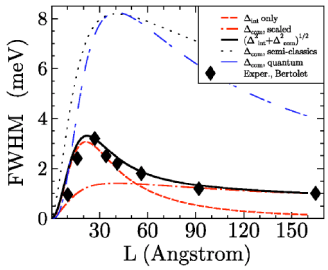

FIG. 8. The thick solid line is the best fit for the total linewidth displayed together with the experimental results (triangles) from Ref. 18. The separate contributions of the interface disorder (Δ_{int}) and of the rescaled alloy disorder (Δ_{alloy}) are also shown. The parameter-free theory for the alloy-disorder contribution discussed in Ref. 13 is shown by the dash-dotted line (without adiabatic approximation). The semiclassical limit of the alloy-disorder contribution (Ref. 3) is shown by the dotted line. The fitted parameters are $\sigma_{||}=3a_{lat}$, $\sigma_\perp=1a_{lat}$.

affect the height, but not the position of the maximum and the shape of the curve. A comparison with the experimental data reproduced in this figure shows that an increase in $\sigma_\perp$ drives the curves away from the experimental results. This has to be compared with the results of incorporating the interwall correlations (Fig. 7). An increase in $\sigma_{||}$ not only significantly reduces the height of the curve maximum, but also shifts its position toward larger values of L and widens it.

It would be interesting to try to fit the experimental data presented in Fig. 1 with the results of our calculations. To this purpose one also needs to know the contribution of the alloy disorder to the total linewidth. Making use of the model of short-range compositional disorder in a QW[13] without the adiabatic approximation, one can obtain the following formula[3] for the alloy-disorder-induced variance W^2:

$$\frac{a_{lat}^3 x(1-x)}{8\pi\lambda^2}\left[\frac{\alpha_h^2}{\beta_e^2}\int_{-L/2}^{L/2}\chi_h(z)^4dz+8\alpha_h\alpha_e \times\int_{-L/2}^{L/2}\chi_h(z)^2\chi_e(z)^2dz+\frac{\alpha_e^2}{\beta_h^2}\int_{-L/2}^{L/2}\chi_e(z)^4dz\right], \quad (36)$$

where a_{lat} is the lattice constant and $\alpha_{e,h}=dV_{e,h}/dx$ characterizes the rate of the shift of the conduction and valence bands with the composition, x. The formula is given for the case of a QW made of a ternary alloy. The semiclassical theory of the exciton linewidth again yields $\Delta=2\sqrt{2\ln(2)}W$, while the interpolation procedure for the quantum limit[13] in effective atomic units[40] gives $\Delta\approx 0.59MW^2$. The $In_{0.12}Ga_{0.88}As/GaAs$ QW is intermediate between these two limits, since $\nu\sim 1$. In Fig. 8 we present both of the Δ dependencies on the well thickness. Unfortunately, as we can see, there exists a strong discrepancy between the theoretical estimates of the contribution from the alloy disorder and the experimental results. Note that Eq. (36) has two enhancement factors. The first one is determined by the lateral shrinkage of the quasi-two-dimensional Bohr's radius of the exciton ($0.5<\lambda<1$). Another stronger enhancement parameter, $1/\beta_e^2=(M/m_e)^2$, is due to heavy hole's mass. It is not the goal of this paper to uncover the causes of this discrep-

ancy. However, common wisdom tells us that in the bulk limit of a very wide QW ($L > a_B$) only alloy-disorder contribution should survive. The simplest way to adjust the theory is to introduce a phenomenological scaling down of Δ_{comp} to the value that should coincide with the experimental results in the limit of the large L asymptote. Although at present the reason for such rescaling is unknown, it is hard to imagine that the proper theory of alloy-disorder contribution will change the dependence of the variance on the well thickness L determined by the integrals in Eq. (36). Since our main purpose is to elucidate the role of the interwall correlations rather than to revise the existing theories of the alloy disorder, we carry out this operation, keeping in mind its purely technical nature. The results of the best fit performed in this way are shown in Fig. 8 along with the best fit values of the lateral and vertical correlation lengths. Performing a similar fitting procedure for other experimental dependencies of the FWHM on well thickness (shown in Fig. 1) we obtained the following values (normalized on lattice constant a_{lat}) for the lateral and inter wall correlation lengths in $In_xGa_{1-x}As/GaAs$ QWs: for $x=0.09$ $\sigma_\perp=1$, $\sigma_{||}=20$, for $x=0.18$ $\sigma_\perp=1$, $\sigma_{||}=10$, for $x=0.11$ $\sigma_\perp=1$, $\sigma_{||}=5$, for $x=0.12$ $\sigma_\perp=1$, $\sigma_{||}=3$, for $x=0.135$ $\sigma_\perp=4$, $\sigma_{||}=13$. The most important result of this exercise is the demonstration that the fit would not be possible at all without taking into account the interwall correlations. We would also like to stress that it is not possible to achieve a good agreement with the experimental results by omitting the interwall correlations and using only the alloy-disorder scaling as an additional fitting parameter. We conclude, therefore, that the interwall correlations play an important role and must be taken into account when interpreting the experimental results.

V. CONCLUSION

In conclusion, in this paper we address the influence of vertical interwall correlations between the rough interfaces on the exciton line shape. We show that the presence of these correlations strongly suppresses the interface-disorder contribution into an inhomogeneous broadening. The latter means that for narrow quantum wells it might happen that the exciton linewidth tells more about the quality of the barrier material than about the quality of the interface, contrary to what is often claimed in the experimental literature. On the other hand, the differences in the interwall correlation lengths can account for the variety of the positions, strengths, and sharpness of the FWHM dependence on the well width for experimental data obtained by different research groups.

ACKNOWLEDGMENTS

We are grateful to S. Schwarz for reading and commenting on the manuscript. The work is supported by AFOSR Grant No. F49620-02-1-0305 and PSC-CUNY research grants.

APPENDIX: DEPENDENCE OF THE LATERAL CORRELATION FUNCTION ON *R*

The calculation of the exciton absorption line shape is equivalent in the dipole approximation to the estimation of the optical density function,[1]

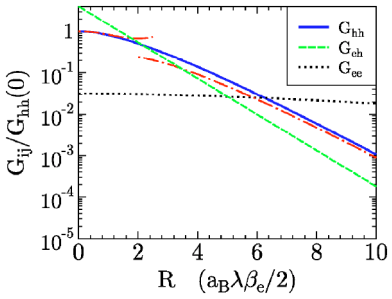

FIG. 9. Semilog arithmic plot of the normalized lateral correlation functions $G_{ij}(R;y_j,\alpha)$. The normalization is chosen in a way to have the hole-hole correlator equal to unity at $R=0$. Data are given for $y_h=0.1$. The ratio $m_e/m_h=0.178$ was chosen to depict the realistic case of the InGaAs/GaAs QW. The dotted-dashed lines for the hole-hole correlator are limits of small and large $\tilde{R}$ [see Eq. (A5)].

$$A(\varepsilon)=\left\langle \sum_i \left| \int d^2R\psi_i(\mathbf{R}) \right|^2 \delta(\varepsilon-\varepsilon_i) \right\rangle, \qquad \text{(A1)}$$

where ε_i and $\psi_i(R)$ are the corresponding energy and wave functions of the Schrödinger equation (8) for the exciton's COM. The shape of $A(\varepsilon)$ depends on the strength of the disorder. The latter can be roughly measured by the parameter $\nu=W/K_c$, where $W=\sqrt{\langle U_{eff}(R)^2\rangle}$ is a variance of the potential energy induced by fluctuations, and $K_c=\hbar^2/2M\ell_c^2$ is the kinetic ("correlational") energy of the exciton. The parameter ℓ_c determines the confinement of the exciton's COM wave function. It can be extracted from the knowledge[15] of the lateral dependence on R for the correlation functions $G_{ij}(R,y_j,\alpha)$ since

$$\ell_c^D=\int d^DR'\langle U(\mathbf{R})U(\mathbf{R}-\mathbf{R}')\rangle/W^2. \qquad \text{(A2)}$$

For the "white-noise" height-height correlator (7) one can show that all of the distances are scaled by factors $(\lambda\beta_i)/2$, i.e., $\tilde{R}=2R/(\lambda\beta_i)$. For the cross-term correlator in the limit of heavy holes and light electrons the result is simple again,

$$G_{eh}(R;y_h,\alpha)\approx G_{eh}(R;y_h,0)=2y_h^2\exp(-\tilde{R}), \qquad \text{(A3)}$$

while for the diagonal terms we have $G_{ii}(R;y_j,0)=y_j^2/2f(\tilde{R}_i)$, where

$$f(\tilde{R})=\frac{4}{\pi}\int_0^\pi d\theta\int_0^\infty d\rho\rho\exp(-\rho-\sqrt{\tilde{R}^2-2\rho\tilde{R}\cos\theta+\rho^2}). \qquad \text{(A4)}$$

The function $f(\tilde{R})$ has the following limits for small and large distances:

$$f(\tilde{R}) \approx \begin{cases} 1 - \frac{1}{4}\tilde{R}^2 + \frac{1}{12}\tilde{R}^3, & \tilde{R} < 1 \\ \sqrt{\frac{\pi\tilde{R}^3}{8}} \exp(-\tilde{R}), & \tilde{R} \gg 1. \end{cases} \quad \text{(A5)}$$

Thus, even though the initial correlator of the interface fluctuations was of the white-noise type, the effective noise for the exciton potential is colored with exponential tails and with a correlation length of the order of the exciton radius. Similar results were obtained earlier for the bulk compositional fluctuations[36] and for the island model of interfacial roughness.[6] One can show that such exponential asymptotes also persist for the long-range Gaussian correlator [Eq. (6)] when $R/y \gg 1$. Since

$$G_{ee}(R) = \left(\frac{m_e}{m_h}\right)^2 G_{hh}\left(R\frac{m_e}{m_h}\right), \quad \text{(A6)}$$

we can see that the lateral part of the electron-electron correlation function is suppressed by the factor $(m_e/m_h)^2$, but it has a larger correlation length. Overall, the localization length ℓ_c is determined however by the hole-hole term $\ell_c \sim \lambda\beta_e$. The normalized lateral correlation functions $G_{ij}(R)$ are shown in Fig. 9.

*Electronic address: ilya@bloch.nrl.navy.mil

[1] A. L. Efros and M. E. Raikh, in *Optical Properties of Mixed Crystals*, edited by R. J. Elliott and I. P. Ipatova (North-Holland, Amsterdam, 1988), p. 133.

[2] C. Weisbuch, R. Dingle, A. Gossard, and W. Wiegmann, Solid State Commun. **38**, 709 (1981).

[3] R. Zimmermann, F. Grosse, and E. Runge, Pure Appl. Chem. **69**, 1179 (1997).

[4] R. Zimmermann, Phys. Status Solidi B **173**, 129 (1992).

[5] V. Srinivas, J. Hryniewicz, Y. J. Chen, and C. E. C. Wood, Phys. Rev. B **46**, 10 193 (1992).

[6] H. Castella and J. W. Wilkins, Phys. Rev. B **58**, 16 186 (1998).

[7] Y. Yayon, A. Esser, M. Rappaport, V. Umansky, H. Shtrikman, and I. Bar-Joseph, Phys. Rev. Lett. **89**, 157402 (2002).

[8] T. A. Germer, Phys. Rev. Lett. **85**, 349 (2000).

[9] V. Holý and T. Baumbach, Phys. Rev. B **49**, 10 (1994).

[10] E. A. Kondrashkina, S. A. Stepanov, R. Opitz, M. Schmidbauer, R. Kohler, R. Hey, M. Wassermeier, and D. V. Novikov, Phys. Rev. B **56**, 10 469 (1997).

[11] D. Bimberg, M. Grundmann, and N. Ledentsov, *Quantum Dot Heterostructures* (John Wiley & Sons, Chichester, 1999).

[12] S. Baranovskii and A. Efros, Sov. Phys. Semicond. **12**, 1328 (1978).

[13] A. L. Efros, C. Wetzel, and J. M. Worlock, Phys. Rev. B **52**, 8384 (1995).

[14] M. Herman, D. Bimberg, and J. Christen, J. Appl. Phys. **70**, R1 (1991).

[15] E. Runge, in *Solid State Physics*, edited by H. Ehrenreich and F. Spaepen (Academic, San Diego, 2002).

[16] A. Patanè, A. Polimeni, M. Capizzi, and F. Martelli, Phys. Rev. B **52**, 2784 (1995).

[17] P. B. Kirby, J. A. Constable, and R. S. Smith, Phys. Rev. B **40**, 3013 (1989).

[18] D. Bertolet, J.-K. Hsu, K. M. Lau, E. Koteles, and D. Owens, J. Appl. Phys. **64**, 6562 (1988).

[19] J.-P. Reithmaier, R. Höger, and H. Riechert, Phys. Rev. B **43**, 4933 (1991).

[20] S. K. Lyo, Phys. Rev. B **48**, 2152 (1993).

[21] M. E. Raikh, N. N. Ablyazov, and A. L. Efros, Sov. Phys. Solid State **25**, 199 (1983).

[22] J. Singh and K. K. Bajaj, J. Appl. Phys. **57**, 5433 (1985).

[23] R. Zimmermann, J. Cryst. Growth **101**, 346 (1990).

[24] H. Zhao, S. Moehl, and H. Kalt, Phys. Rev. Lett. **89**, 097401 (2002).

[25] D. Bimberg, D. Mars, J. Miller, R. Bauer, and D. Oertel, J. Vac. Sci. Technol. B **4**, 1014 (1986).

[26] A. Ourmazd, D. W. Taylor, J. Cunningham, and C. W. Tu, Phys. Rev. Lett. **62**, 933 (1989).

[27] J. Christen, M. Grundmann, and D. Bimberg, Appl. Surf. Sci. **41–42**, 329 (1989).

[28] J. Singh, K. K. Bajaj, and S. Chaudhri, Appl. Phys. Lett. **49**, 805 (1984).

[29] A. E. Meyerovich and A. Stepaniants, Phys. Rev. B **58**, 13 242 (1998).

[30] A. E. Meyerovich and A. Stepaniants, Phys. Rev. B **60**, 9129 (1999).

[31] A. E. Meyerovich and I. V. Ponomarev, Phys. Rev. B **65**, 155413 (2002).

[32] G. Bastard, E. E. Mendez, L. L. Chang, and L. Esaki, Phys. Rev. B **26**, 1974 (1982).

[33] H. A. Bethe and E. E. Salpeter, *Quantum Mechanics of One and Two Electron Systems* (Springer, Berlin, 1957).

[34] R. Zimmermann, J. Appl. Phys. **34**, 228 (1994).

[35] I. V. Ponomarev, L. I. Deych, V. A. Shuvayev, and A. A. Lisyansky, Physica E (Amsterdam) **25**, 539 (2005).

[36] Z. S. Gevorkyan and Y. E. Lozovik, Sov. Phys. Solid State **27**, 1079 (1985).

[37] I. V. Ponomarev, V. V. Flambaum, and A. L. Efros, Phys. Rev. B **60**, 5485 (1999).

[38] In fact, the value calculated with the help of Eq. (A4) in Ref. 13 would be even smaller, since the authors omitted without any reason the cross term $2\alpha_e\alpha_h \int \chi_e^2\chi_h^2 dz$, which is of the same order of value as the other two terms.

[39] For a detailed derivation of the volume element in the two-dimensional case see Appendix B in Ref. 37.

[40] As stated at the beginning of Sec. III A, all of our formulas are given in effective atomic units, $\hbar = e = \mu = a_B = 1$ Therefore the values W and M are are dimensionless, and the physical magnitude for the width in meV can be obtained by the multiplication of the dimensionless Δ by the three-dimensional (3D) exciton ground-state energy $E_{\text{a.u.}}$ for a given material. In the units of Ref. 13 this formula is, $\Delta \approx 0.59 MW^2/\hbar^2$, where the variance W^2 is given in meV^2 Å^2